Skin tropism during Usutu virus and West Nile virus infection: an amplifying and immunological role

Axelle Vouillon, Jonathan Barthelemy, Lucie Lebeau, Sébastien Nisole, Giovanni Savini, Nicolas Lévêque, Yannick Simonin, Magali Garcia, Charles Bodet

Journal of Virology

Pathogenesis and Host Response | Full-Length Text

Skin tropism during Usutu virus and West Nile virus infection: an amplifying and immunological role

Axelle Vouillon,[1] Jonathan Barthelemy,[2] Lucie Lebeau,[3] Sébastien Nisole,[4] Giovanni Savini,[5] Nicolas Lévêque,[1,6] Yannick Simonin,[2] Magali Garcia,[1,6] Charles Bodet[1]

AUTHOR AFFILIATIONS See affiliation list on p. 12.

ABSTRACT Usutu virus (USUV) and West Nile virus (WNV) are closely related emerging arboviruses belonging to the *Flavivirus* genus and posing global public health concerns. Although human infection by these viruses is mainly asymptomatic, both have been associated with neurological disorders such as encephalitis and meningoencephalitis. Since USUV and WNV are transmitted through the bite of an infected mosquito, the skin represents the initial site of virus inoculation and provides the first line of host defense. Although some data on the early stages of WNV skin infection are available, very little is known about USUV. Herein, USUV-skin resident cell interactions were characterized. Using primary human keratinocytes and fibroblasts, an early replication of USUV during the first 24 hours was shown in both skin cells. In human skin explants, a high viral tropism for keratinocytes was observed. USUV infection of these models induced type I and III interferon responses associated with upregulated expression of various interferon-stimulated genes as well as pro-inflammatory cytokine and chemokine genes. Among the four USUV lineages studied, the Europe 2 strain replicated more efficiently in skin cells and induced a higher innate immune response. *In vivo*, USUV and WNV disseminated quickly from the inoculation site to distal cutaneous tissues. In addition, viral replication and persistence in skin cells were associated with an antiviral response. Taken together, these results provide a better understanding of the pathophysiology of the early steps of USUV infection and suggest that the skin constitutes a major amplifying organ for USUV and WNV infection.

IMPORTANCE Usutu virus (USUV) and West Nile virus (WNV) are closely related emerging *Flaviviruses* transmitted through the bite of an infected mosquito. Since they are directly inoculated within the upper skin layers, the interactions between the virus and skin cells are critical in the pathophysiology of USUV and WNV infection. Here, during the early steps of infection, we showed that USUV can efficiently infect two human resident skin cell types at the inoculation site: the epidermal keratinocytes and the dermal fibroblasts, leading to the induction of an antiviral innate immune response. Moreover, following cutaneous inoculation, we demonstrated that both viruses can rapidly spread, replicate, and persist in all distal cutaneous tissues in mice, a phenomenon associated with a generalized skin inflammatory response. These results highlight the key amplifying and immunological role of the skin during USUV and WNV infection.

KEYWORDS flavivirus, Usutu virus, West Nile virus, keratinocytes, fibroblasts, skin tropism, innate immune response, viral dissemination

In the past three decades, the emergence of arboviruses posed a considerable global health threat (1). Among them, Usutu (USUV) and West Nile (WNV) viruses, two *Flaviviruses* belonging to the Japanese encephalitis virus serocomplex, share many common features (2). After being discovered in Africa, they have spread to other regions:

Editor Christiane E. Wobus, University of Michigan Medical School, Ann Arbor, Michigan, USA

Address correspondence to Charles Bodet, charles.bodet@univ-poitiers.fr.

Magali Garcia and Charles Bodet contributed equally to this article.

The authors declare no conflict of interest.

Received 23 November 2023
Accepted 27 November 2023
Published 13 December 2023

WNV is endemic worldwide, whereas USUV is on the rise in Europe (1). Their transmission cycle involves hematophagous mosquitoes such as *Culex pipiens* as vectors and wild birds as reservoirs (3). Infected mosquitoes can also occasionally transmit these viruses to humans and horses, considered dead-end hosts, but also to dogs, rodents, and deer (3). Mainly asymptomatic or associated with mild symptoms such as fever or rash (4), WNV infection can progress to neuroinvasive disease and has resulted in numerous outbreaks affecting both humans, horses, and birds, while USUV has caused significant avian epizootics in Europe, with over a hundred cases of acute human infection, including neurological disorders (3). Since these viruses are inoculated within the skin through the bite of an infected mosquito, virus/skin cell interactions are critical in the pathophysiology of USUV and WNV infection. The superficial layers of the skin are the epidermis, a stratified epithelium primarily constituted of keratinocytes, and the dermis, made up of connective tissue produced by fibroblasts. Skin innate immune surveillance is ensured by various immune cells, including epidermal Langerhans cells (LCs) and dermal dendritic cells (DCs), as well as non-immune skin-resident cells, such as keratinocytes and fibroblasts (5). By expressing pathogen recognition receptors (PRRs), such as Toll-like receptor 3 (TLR3), Retinoic acid-inducible gene I (RIG-I), and melanoma differentiation-associated gene 5 (MDA5), these cells can recognize viral pathogen-associated molecular patterns (PAMPs) and act as immune sentinels. Pathogen recognition triggers downstream signaling pathways leading to the production of inflammatory mediators, which influence the trafficking and activation of immune cells within the skin, as well as interferon-stimulated genes (ISGs), which are powerful effectors of the antiviral response, or antimicrobial peptides (AMPs) (5).

Very little is known about USUV-skin cell interactions at the inoculation site. While a previous study showed the ability of USUV to replicate in LCs (6), the permissiveness of keratinocytes and fibroblasts to infection and the innate immune response induced remain uncharacterized. In this work, the capacity of USUV to infect human skin cells was evaluated using primary keratinocytes and fibroblast monolayers as well as *ex vivo* human skin explants. Our data demonstrate that human keratinocytes and fibroblasts are permissive to USUV infection resulting in the induction of an antiviral response. Moreover, an *in vivo* mouse model of subcutaneous infection was used to assess the ability of USUV, compared to WNV, to disseminate within the skin tissues. This study shows that both viruses rapidly spread, replicate, and persist in distal cutaneous tissues, suggesting that the skin constitutes an amplifying organ during USUV and WNV infection.

RESULTS

USUV strains differentially replicate in primary human keratinocytes inducing an innate immune response

Considering that infected mosquitoes inoculate USUV within the epidermis during the probing step of blood meal, the susceptibility of primary human keratinocytes to different lineages of USUV was determined. Keratinocytes were infected with four strains of USUV [Europe 2 (EU2), Europe 5 (EU5), Africa 2 (AF2), and Africa 3 (AF3)] at an MOI of 1, and intracellular viral RNA was quantified by RT-qPCR. The amount of viral RNA significantly increased 22-fold at 24 hours post-infection (hpi) in cells infected with the EU2 strain, while the increase in viral loads was less marked during infection with the EU5 and AF2 strains and not observed with the AF3 strain (Fig. 1A). Next, we quantified viral RNA and infectious viral particle production in the supernatants of USUV-infected keratinocytes using RT-qPCR and endpoint dilution assay, respectively. USUV RNA levels of EU2, EU5, and AF2 strains significantly increased, mainly during the first 24 hours of keratinocyte infection (Fig. 1B). Viral titers confirmed the higher capacity of the EU2 strain to replicate in keratinocytes, the production of infectious viral particles being at least 10 times higher compared to the other strains at 24 hpi (Fig. 1C). Among the four strains tested, keratinocytes seemed to be less permissive to AF3 infection .

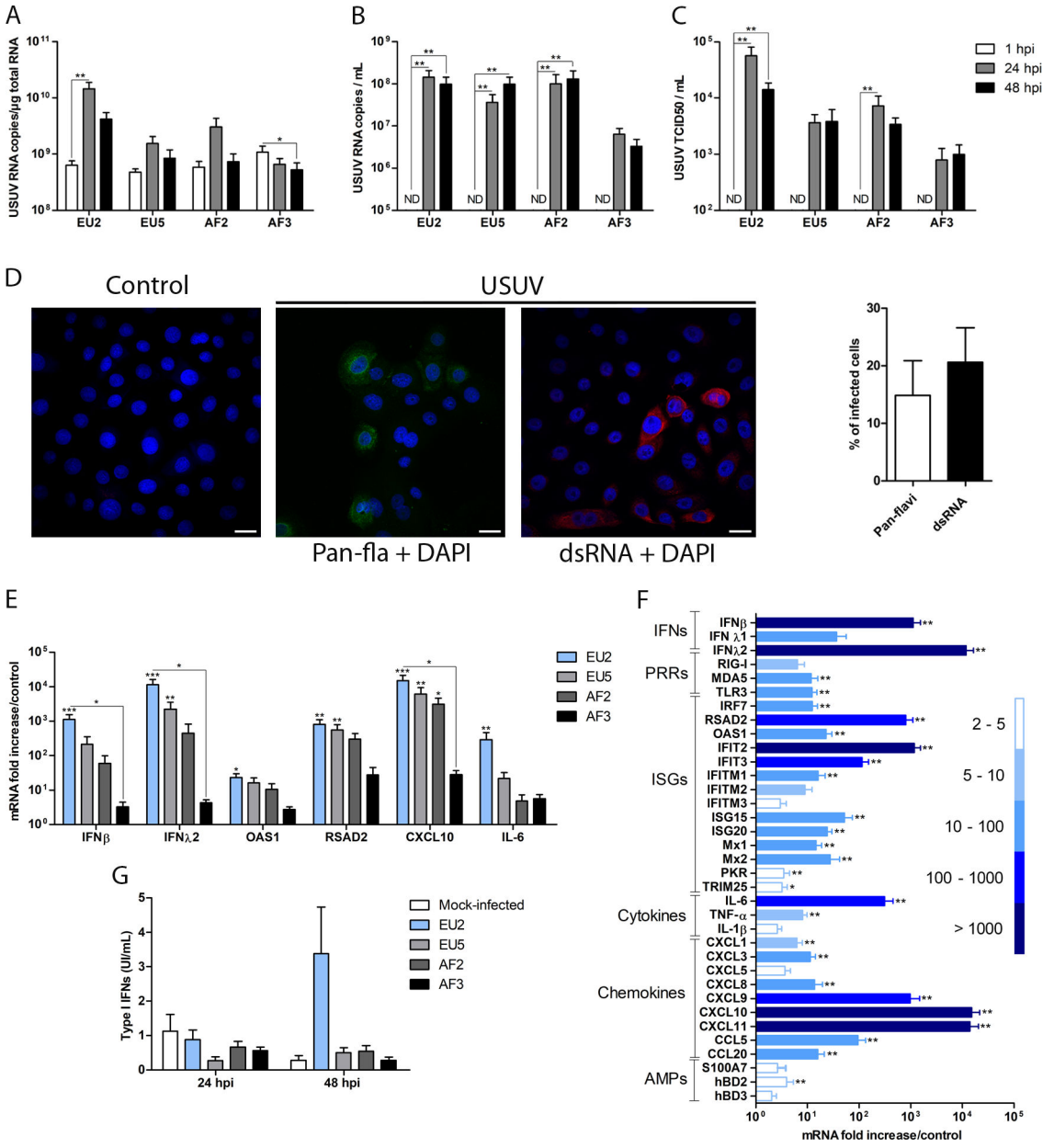

FIG 1 USUV replicates in keratinocytes and induces an innate immune response. Primary human keratinocytes were infected by USUV strains at an MOI of 1. (A) Quantification of viral RNA in cell lysates and (B) in cell supernatant. (C) Quantification of viral particle production in the supernatant using the end-point dilution assay. (D) Left panel: mock and EU2-infected cells were labeled at 24 hpi with pan-*Flavivirus* envelope protein antibody (green), double-stranded RNA (dsRNA) antibody (red), and DAPI (blue) (scale bar = 20 µm). Right panel: quantification of USUV-infected cells at 24 hpi using pan-*Flavivirus* and dsRNA antibodies. (E) Induction of inflammatory and antiviral gene expression in USUV-infected keratinocytes at 24 hpi. (F) mRNA expression of a large panel of IFNs, ISGs, cytokines, and chemokines by keratinocytes infected with EU2 strain at 24 hpi. (G) Secretion levels of type I IFNs by USUV-infected keratinocytes. Data are represented as mean ± SEM of six independent experiments. *$p < 0.05$, **$p < 0.01$, and ***$p < 0.001$. ND, not detected.

In cells infected with EU2 strain, viral envelope protein E and viral double-stranded RNA (dsRNA) replication intermediate production was then evaluated by immunofluorescence at 24 hpi (Fig. 1D). While no staining was observed in mock-infected cells, viral envelope proteins and dsRNA were detected in 15% and 20% of infected keratinocytes, respectively, demonstrating efficient replication and viral protein production.

To determine whether USUV induces an innate antiviral immune response in infected cells, the antiviral and inflammatory gene expression profile was characterized in keratinocytes at 24 hpi (Fig. 1E). A strong upregulation of interferon (IFN)β, IFNλ2,

2′,5′- oligoadenylate synthase (OAS)1, radical S-adenosyl methionine domain-containing protein 2 (RSAD2), C-X-C motif chemokine ligand 10 (CXCL10), and interleukin (IL-6) mRNA expression in infected cells, especially for the EU2 strain, was observed. For example, IFNβ and IFNλ2 mRNA expression enhanced with a fold-change ranging from 10^3 to 10^4 following keratinocyte infection with EU2 strain, whereas only a fourfold increase was observed for the AF3 strain compared to mock-infected cells (Fig. 1E). Next, the ability of EU2 strain to induce mRNA expression of a large panel of PRRs, cytokines, chemokines, ISGs, and AMPs was shown (Fig. 1F). Significant induction of TLR3 and MDA5 mRNA expression, PRRs involved in the detection of other *Flaviviruses* (5), was observed in response to USUV infection. Moreover, the mRNA level of interferon regulatory factor 7 (IRF7), a transcription factor known to mobilize antiviral machinery, increased significantly in USUV-infected cells. In agreement, in addition to RSAD2, OAS1, overexpression of numerous ISGs involved in antiviral defenses (7), including interferon-induced protein with tetratricopeptide repeats (IFIT)2 and IFIT3, interferon-induced transmembrane protein (IFITM)1, IFN-induced gene (ISG)15, ISG20, myxovirus resistance protein (MX)1 and MX2, protein kinase R (PKR), and tripartite motif-containing protein 25 (TRIM25), was also significantly induced by infection. This antiviral response was associated with significantly enhanced expression of pro-inflammatory cytokines, such as tumor necrosis factor (TNF)-α and IL-6, and chemokines, such as CXCL1/3/8/9/10/11, C-C motif chemokine ligand (CCL)5, and CCL20. The most induced inflammatory mediators were CXCL10 and CXCL11 with a fold-change higher than 1,000. Finally, keratinocytes are known to secrete AMPs that can exert antiviral activities (8). Our results showed a significant induction of the human β-defensin-2 mRNA expression. At the protein level, enhanced production of type I IFNs was only observed with EU2 strain at 48 hpi (Fig. 1G). The apparent discrepancy between the mRNA expression level and the secreted amount of biologically active type I IFNs may be due to their very short half-life as well as autocrine and paracrine consumption of IFNs produced as suggested by the significant induction of expression of numerous ISGs observed.

Primary human fibroblasts are also permissive to USUV infection

Since infected mosquitoes also inoculate the virus in the extravascular space of the dermis, we hypothesized that dermal fibroblasts could be another target for USUV. Primary human fibroblasts were infected with USUV EU2 and AF2 strains at a MOI of 1 over a course of 48-hour infection. A significant increase of intracellular viral RNA was found in USUV-infected fibroblasts from 24 hpi, with a fold change ranging from 22 to 53 for the AF2 and EU2 strains, respectively (Fig. 2A). Viral quantification and titration in supernatants showed significant production of viral RNA and infectious particles mostly occurring during the first 24 hours of infection for both strains (Fig. 2B and C). When staining for envelope protein and dsRNA, about 50% of cells infected with EU2 strain was found positive for both targets, highlighting a higher infection rate in fibroblasts than in keratinocytes (Fig. 2D). Then, the innate immune response of USUV-infected fibroblasts was investigated. IFNβ, IFNλ2, OAS1, RSAD2, CXCL10, and IL-6 mRNA levels were significantly increased almost similarly by both strains. Among them, CXCL10 mRNA was the most induced at levels around 20,000-fold in EU2-infected cells compared to mock-infected cells. Moreover, EU2 induced significant and strong secretion of type I IFNs compared to AF2 by infected fibroblasts at 48 hpi. These results provide evidence that USUV can infect and replicate in fibroblasts as well as to induce an intense pro-inflammatory and antiviral response.

USUV replicates in an *ex vivo* human skin model and induces an inflammatory response

To mimic the viral inoculation by mosquitoes, the USUV EU2 strain was injected into human skin explants. The amount of viral RNA at the inoculation site was slightly increased during the first 24 hpi before decreasing at 48 hpi (Fig. 3A). In contrast, viral RNA levels (Fig. 3B) and infectious particles (Fig. 3C) in the culture medium significantly

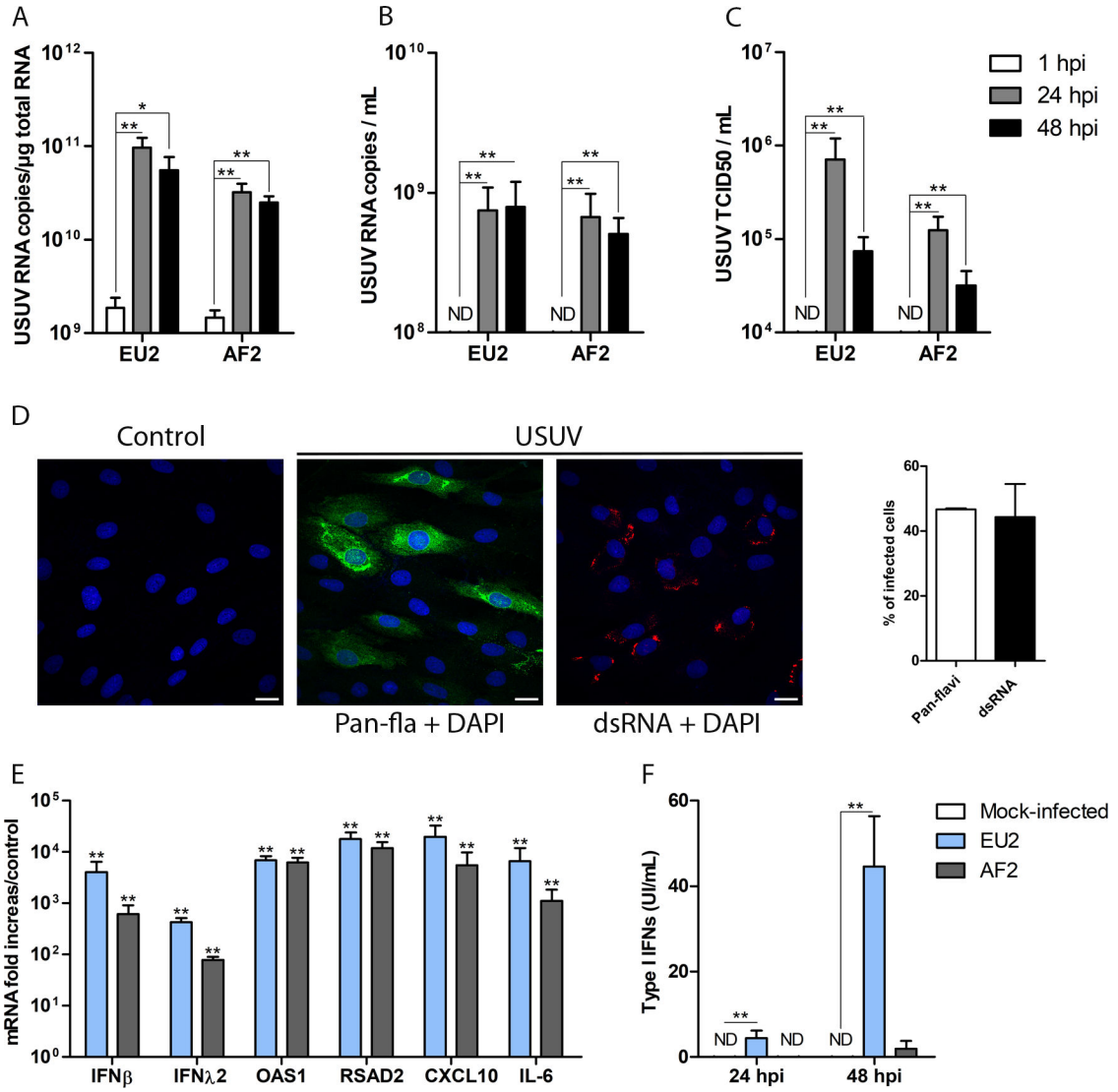

FIG 2 USUV replicates in fibroblasts and induces an innate immune response. Primary human fibroblasts were infected by USUV at a MOI of 1. (A) Quantification of viral RNA in cell lysates and (B) cell supernatant. (C) Quantification of viral particle production in the supernatant using the end-point dilution assay. (D) Left panel: mock and EU2-infected cells were labeled at 24 hpi with pan-*Flavivirus* envelope protein antibody (green), dsRNA antibody (red), and DAPI (blue) (scale = 20 µm). Right panel: quantification of USUV-infected cells at 24 hpi using pan-*Flavivirus* or dsRNA antibodies. (E) Induction of inflammatory and antiviral gene expression in USUV-infected fibroblasts at 24 hpi. (F) Secretion levels of type I IFNs by USUV-infected fibroblasts. Data are represented as mean ± SEM of six independent experiments. *$p < 0.05$ and **$p < 0.01$. ND, not detected.

increased at 24 hpi and up to 48 hpi. Furthermore, at 24 hpi, dsRNA replication intermediates were detected primarily throughout the epidermis and only at a few rare locations in the extravascular space of the dermis, whereas viral envelope protein was detected mainly from scattered locations within the epidermis (Fig. 3D). Co-immunostaining of dsRNA with cytokeratin 10 (CK10), a marker of differentiated keratinocytes not expressed by basal keratinocytes, confirmed that keratinocytes from the basal to suprabasal layers of the epidermis are the main target of USUV in infected skin. The specificity of viral replication intermediate staining was validated by labeling an uninfected skin explant with the anti-dsRNA antibody (Fig. S1). Moreover, mRNA expression levels of pro-inflammatory and antiviral genes were monitored (Fig. 3E). At 24 hpi, expression of IFNβ mRNA was significantly increased approximately 20-fold as well as mRNA of several ISGs, such as RSAD2 and MX1, with fold change higher than 80. Finally,

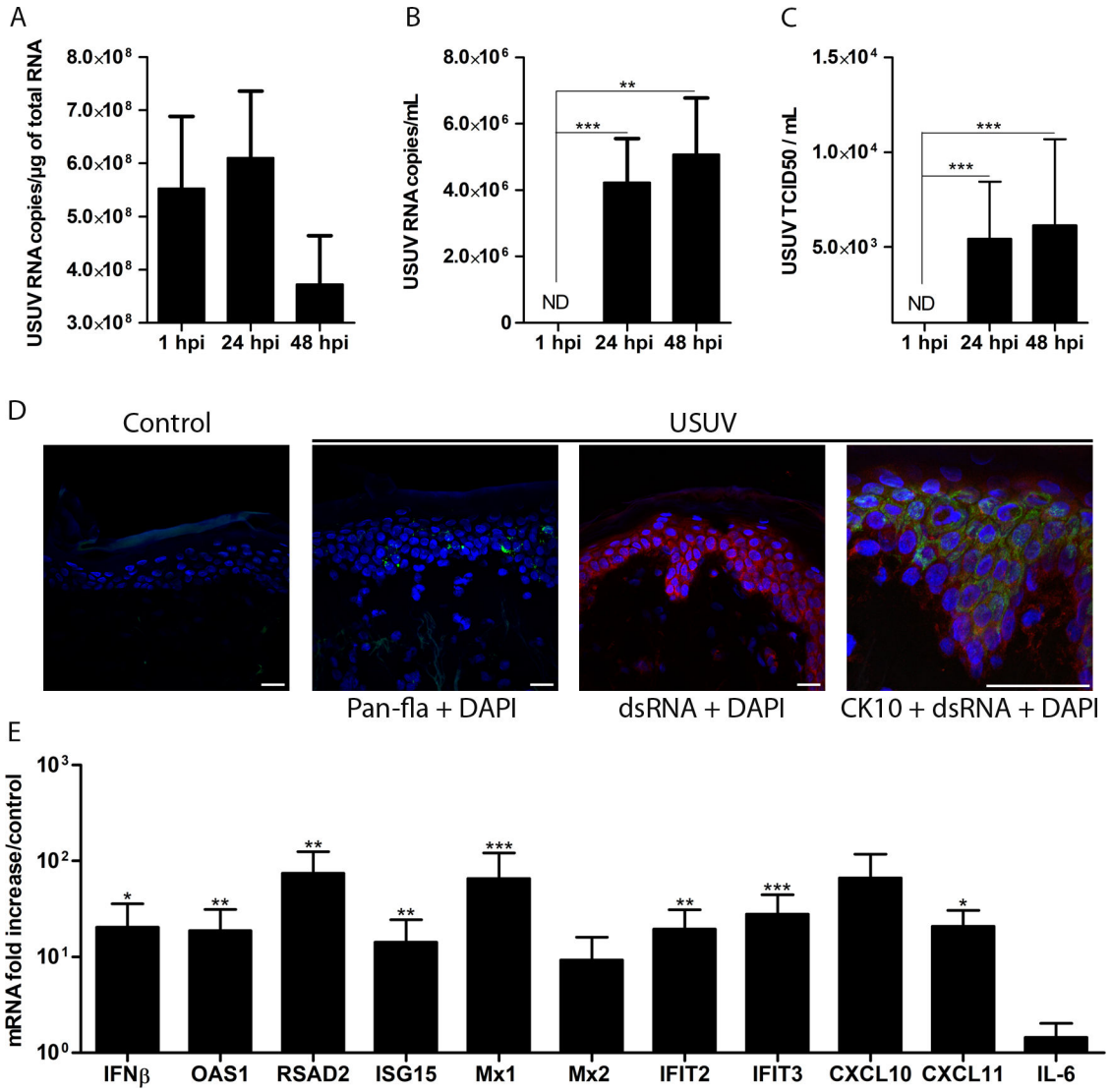

FIG 3 USUV infection of human skin explants. Skin was infected intradermally with the USUV EU2 strain. (A) Quantification of viral RNA at the inoculation site biopsies and (B) cell culture supernatants at 1, 24, and 48 hpi. (C) Quantification of infective viral particle production in the supernatants using the end-point dilution assay. (D) Skin biopsies were labeled at 24 hpi with pan-*Flavivirus* envelope protein antibody (green), dsRNA antibody (red), CK10 (green), and DAPI (blue) (scale = 20 µm). (E) mRNA expression of IFNs, ISGs, cytokines, and chemokines at 24 hpi. Data are represented as mean ± SEM of five independent experiments performed in duplicate. *$p < 0.05$, **$p < 0.01$, and ***$p < 0.001$. ND, not detected.

mRNA expression of CXCL11 significantly increased during USUV infection, whereas IL-6 remained near basal expression levels (Fig. 3E).

Dissemination and persistence of USUV and WNV infection in cutaneous tissues

To our knowledge, the ability of USUV to infect and disseminate in cutaneous tissues *in vivo* has not been studied so far. As immunocompetent adult mice do not appear susceptible to USUV infection (9), we used neonatal immunocompetent mice, a model previously demonstrated as permissive (10), up to 6 days post-infection (dpi). For comparison with a closely related *Flavivirus*, mice were infected with WNV using the same protocol except that the experiment was stopped at 5 dpi because of the onset of neurological symptoms, reflecting higher virulence of WNV in this model. Suckling mice were subcutaneously infected with the USUV EU2 strain or WNV lineage 2 (L2) strain on

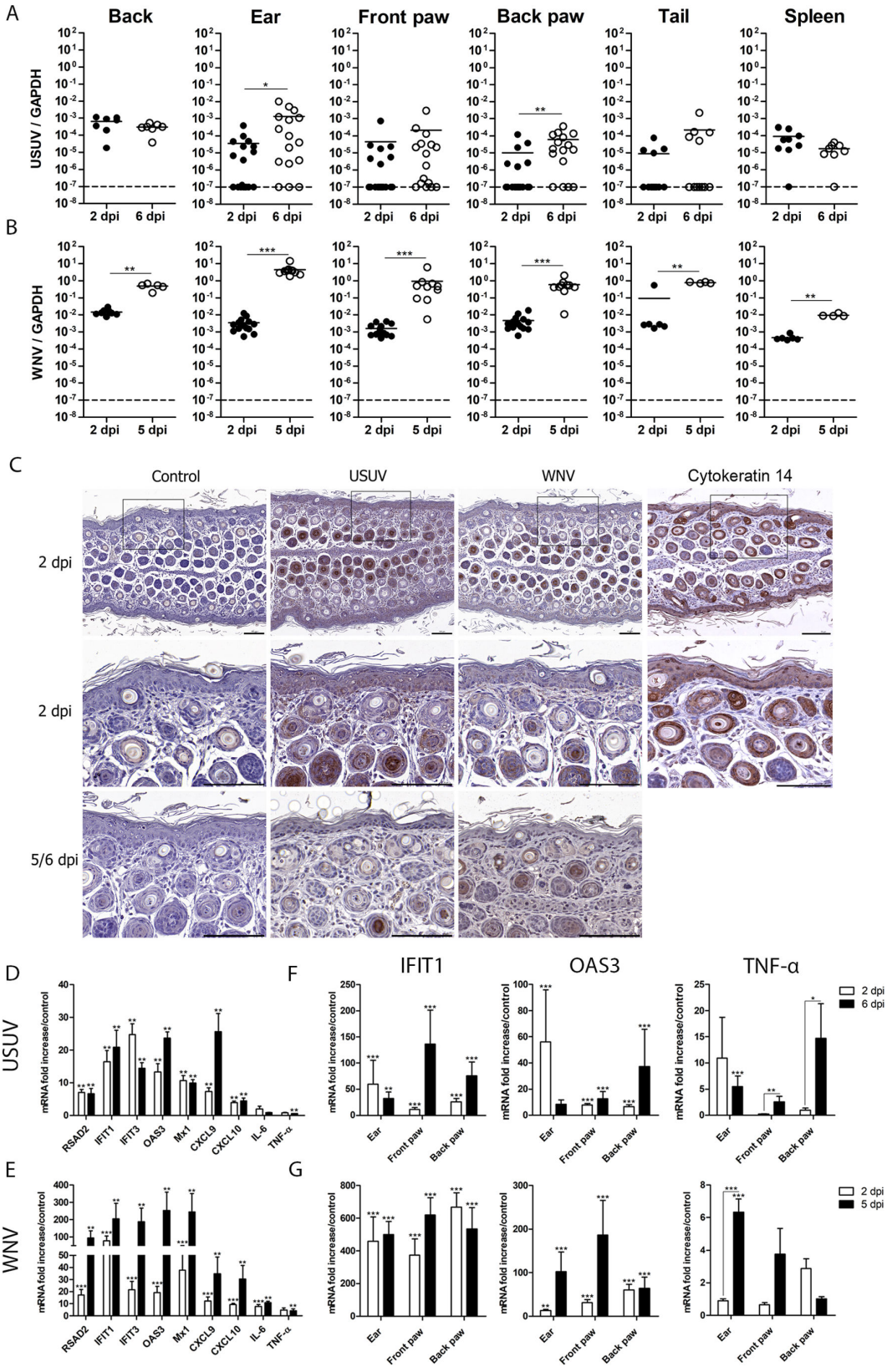

FIG 4 Replication, dissemination, and persistence of USUV and WNV in skin tissues. Mice were infected subcutaneously with USUV or WNV in the back. (A) Viral RNA was quantified at 2 and 6 dpi for USUV and (B) at 2 and 5 dpi for WNV. (C) Transverse sections of the ears of mock-, WNV-, or USUV-infected mice showing detection of viral dsRNA and cytokeratin 14 (scale = 100 µm). mRNA fold increase of ISGs, cytokines, and chemokines from skin of the back (D and E) or in distal limbs (F and G) of infected mice as compared to mock-infected controls. *$p < 0.05$, **$p < 0.01$, and ***$p < 0.001$. ND, not detected.

the back. Spleen and cutaneous tissues from the inoculation site (back), the ears, the paws, and the tail were harvested at each time point.

We first quantified the amount of viral RNA in different tissues (Fig. 4A and B). USUV and WNV RNA were detected at the inoculation site at 2 dpi in all mice. While RNA levels remained similar at 6 dpi for USUV, they continued to significantly increase up to 5 dpi for WNV. Furthermore, USUV RNA was detected in distal cutaneous tissues from the inoculation site from 2 dpi, the percentage of positive samples varying between 30 and 55 depending on the location (ears: 55%, front paws: 38%, back paws: 33%, and tails: 30%). These amounts of USUV RNA were significantly increased at 6 dpi in the skin of ears and back paws, in agreement with higher percentages of EU2-infected skin tissues found in ears (80%), front and back paws (75%), and tails (42%). USUV RNA was also detected in the spleen at 2 and 6 dpi, with 88% of positive samples at 6 dpi. In comparison, WNV RNA was detected in all distal cutaneous tissues and spleen from 2 dpi with higher amounts than USUV. At 5 dpi, we noticed a significant increase in WNV RNA amounts in all cutaneous tissues and spleen. Immunostaining of dsRNA in ear skin confirmed *in situ* replication in distal cutaneous tissues and was mainly located in the epidermis and hair follicles, especially in areas containing cytokeratin 14-positive cells, a marker of proliferative keratinocytes, suggesting USUV and WNV replication primarily in epithelial tissues (Fig. 4C). Taken together, these results show that USUV and WNV share a tropism for cutaneous tissues and that the skin is a site of viral dissemination and constitutes an amplifying organ during infection by these viruses.

We then investigated the effect of USUV and WNV infection on gene expression of some key host antiviral proteins or pro-inflammatory mediators, not only at the inoculation site but also in distal cutaneous tissues. At the inoculation site, mRNA expression levels of ISGs, such as RSAD2, IFIT1/3, OAS3, and MX1, and the chemokines CXCL9 and CXCL10 were significantly enhanced by both viruses (Fig. 4D and E). Regarding pro-inflammatory cytokines, IL-6 mRNA expression was induced only by WNV, while TNF-α mRNA expression was significantly enhanced following infection with WNV and USUV at 5 and 6 dpi, respectively. If a similar trend was found at the inoculation site at 2 dpi for both viruses, at late times of infection, mRNA levels of ISGs were at least 10-fold higher in mice infected by WNV compared to USUV (Fig. 4E). Finally, in distal cutaneous tissues, mRNA levels of OAS3 and IFIT1 were upregulated after infection by USUV (Fig. 4F) and WNV (Fig. 4G), WNV still inducing a higher mRNA expression of these mediators. Enhanced mRNA expression of TNF-α was only observed in ears for both viruses at late times of infection. Overall, compared to USUV, both tissular viral loads and intensity of host response were higher during WNV infection. These results show that USUV and WNV replication was associated with a pro-inflammatory and antiviral response in infected cutaneous tissues.

DISCUSSION

Arboviruses, such as Zika, dengue (DENV), WNV, or USUV, represent a significant global health concern due to their spread enabled by a wider distribution of mosquito vectors caused by global warming (1). Following their inoculation, the skin is the first site of viral replication and initiation of the innate immune response (5). Non-immune resident skin cells, i.e., epidermal keratinocytes and dermal fibroblasts, are known to play a key role in the early steps of infection by *Flaviviruses* (11–16). Regarding USUV, its ability to infect these cells had not yet been investigated, as only LCs had previously been shown to be permissive to USUV infection in the skin (6). Our study shows that primary human epidermal keratinocytes and dermal fibroblasts supported a fast and strong replication of different USUV strains. In addition, using a more complex *ex vivo* model, USUV dsRNA replication intermediates were detected mainly in the epidermis but also in the dermis of human skin explant, and viral envelope proteins were localized in the epidermis. These results suggest that keratinocytes and fibroblasts are major target cells of USUV, the virus exhibiting higher tropism for both basal and differentiated keratinocytes in human skin tissue. We also noticed different replication profiles between USUV strains. In particular,

the EU2 isolate replicated most efficiently in both cell types, whereas keratinocytes seem to be less permissive to infection with the AF3 strain. This is in agreement with previous work reporting that the EU2 strain was more virulent in mice and neurotropic since it replicated more easily in neuronal cells compared to the AF3 isolate (17). In fact, an amino acid substitution specific to the RNA-dependent RNA polymerase domain of the non-structural protein 5 may be involved in the better efficiency of USUV EU2 replication (17, 18).

The outcome of a viral infection depends on the winner of the competition between viral replication and host antiviral immune response. Our results showed that USUV replication in skin cells occurs mainly during the first 24 hours of infection before the innate immune response is set up. A correlation between levels of viral replication and host response in keratinocytes and fibroblasts was observed. Indeed, USUV EU2, the strongest replicating strain, was also a more potent inducer of antiviral cytokines and chemokines, including type I and III IFNs. In agreement with the findings of Martin et al. (6), it appears that USUV and the IFN response are engaged in a race, where the virus attempts to replicate rapidly before the establishment of an efficient cellular antiviral state induced by IFNs. Otherwise, compared to WNV, previous studies showed that USUV induces a stronger type I and III IFNs' response in LCs and DCs and is more susceptible to type I and III IFN pretreatment (6, 19). Unlike some other *Flaviviruses*, USUV seems to possess a poor ability to evade IFN-associated innate immunity and to counteract host antiviral cellular defense.

The immune system is designed to quickly regulate viral replication and restrict the spread of the virus by sensing viral PAMPs, which then trigger the antiviral response. Indeed, infection of human keratinocytes with USUV increased the expression of several antiviral gene clusters, including PRRs, such as RIG-I, MDA5, and TLR3, which can recognize viral PAMPs from other *Flaviviruses*, such as DENV and WNV (13, 20). In addition, skin cell infection by USUV resulted in an enhanced mRNA level of type I and III IFNs and IRF7, a transcription factor that promotes IFN expression (21). Coherently, upregulation of mRNA expression of various ISGs, including RSAD2, OAS1, IFIT2-3, IFITM1-3, ISG15, ISG20, MX1-2, PKR, and TRIM25, was induced by USUV. While WNV restriction by some of these ISGs is characterized, nothing has yet been published on their role against USUV (7). For example, RSAD2, also known as viperin, interferes with WNV replication by inhibiting RNA transcription and the assembly and budding of immature virions (22). Otherwise, OAS1 contributes to WNV restriction by degrading the viral genome into small RNAs, permitting their sensing by RIG-I and MDA5 (7), and a single nucleotide polymorphism in the OAS1 gene has been identified as a genetic risk factor for human WNV infection (23). Although USUV restriction factors remain to be identified, the strong induction of ISGs in infected skin cells can exert an antiviral role against USUV. This could explain the rapid blocking of viral replication observed in cell monolayers, whereas in more complex models, such as human skin explant and mouse skin, viruses could still spread to areas where the innate response would not have yet been triggered.

In addition, USUV infection of skin cells induces the expression of various cytokines and chemokines, such as IL-6, TNF-α, and CXCL10, which are known to play a key role in the host inflammatory and immune response to flaviviral infection in other cell types (10, 17, 24). This underscores the importance of keratinocytes and fibroblasts as innate immune sentinels capable of initiating a cutaneous antiviral response and attracting various types of leucocytes at the site of infection. However, the impact of the cutaneous cytokine response on the course of USUV infection remains to be determined. Indeed, for WNV, inflammatory mediators exert a multifaceted role in viral pathogenesis through the modulation of viral replication and immune-mediated tissue damage, with some cytokines providing protection against acute infection, while others can have both protective and deleterious effects (24).

Considering the ability of USUV and WNV to infect skin cells, viral dissemination and persistence in cutaneous tissues, including remotely from the inoculation site, were

explored using a mouse model. Through subcutaneous inoculation, close to the natural route of infection, we demonstrated that USUV and WNV can quickly disseminate from the inoculation site to distal cutaneous tissues, where the viral load tended to increase during the kinetics of infection. Moreover, the increase of viral RNA and detection of dsRNA replication intermediates in the ear skin in the course of infection indicate that USUV and WNV can replicate in cutaneous tissue before the onset of neurological signs and underline the importance of the skin in virus amplification during systemic dissemination. Furthermore, viral replication in skin-distal sites was observed in the epidermis and adnexal glands, as previously reported in the footpad skin inoculation site of WNV-infected mice (12), highlighting the fact that both viruses possess strong tropism for keratinocytes *in vivo*. By emphasizing the determining role of the initial stages of cutaneous viral replication during infection with other *Flaviviruses*, previous studies have shown that removing the skin inoculation site, after several hours of infection, rescued mice from disease (25, 26). Taken together, these results underscore the importance of the skin during the early steps of *Flavivirus* pathophysiology and their dissemination through the host.

To date, USUV pathogenesis remains largely unknown. Because USUV is phylogenetically close to WNV, it can be assumed that USUV pathogenesis has similarities to WNV. After cutaneous inoculation, WNV replicates in resident skin cells, such as keratinocytes, fibroblasts, and DCs, then migrates to the draining lymph nodes, and spreads to peripheral organs including the spleen and brain. We detected USUV in the spleen at 2 dpi, suggesting that USUV is disseminated quickly through the blood during the first days, leading to infection of several peripheral organs from the inoculation site to distal cutaneous tissues. However, we observed significantly more viral RNA in cutaneous tissues and spleen of WNV-infected mice compared to USUV. This can be due to virulence factors and immune escape mechanisms of WNV (7), which could explain its stronger pathogenicity in mouse models compared to USUV. Finally, the persistence of USUV and WNV infection in cutaneous tissue was observed up until 5- and 6-days post-infection, respectively. The ability of WNV to persist in cutaneous tissue was previously demonstrated in sparrows (27) and mice (28) from 1 to 4 months post-inoculation. These findings suggest that skin can be a reservoir for flavivirus spread.

As a whole, our results demonstrate the susceptibility of keratinocytes and fibroblasts to USUV infection and their ability to initiate an antiviral response. However, despite this antiviral response, the virus was able to replicate, disseminate, and persist in cutaneous tissues, thus illustrating some ability of USUV to escape skin immune defenses. Taken together, this highlights the pivotal role of the skin in the pathophysiology of USUV. Furthermore, during blood feeding, mosquitoes co-inoculate virus and saliva within the skin. As the mosquito salivary components are known to be critical for the pathogenesis of flavivirus infection, further investigations are needed to study the impact of mosquito saliva on USUV skin infection.

MATERIALS AND METHODS

Viruses and reagents

USUV and WNV strains (detailed in Table S1) were amplified on the C6/36 cells (ATCC CRL-1660), as previously described (29). Viral titers were determined on Vero cells using the Spearman-Kärber method (11). The reagents used in this work are listed in Table S2.

Infection of normal human epidermal keratinocytes and dermal fibroblasts

Primary keratinocytes and fibroblasts were isolated from human skin and cultured as previously described (11, 30). Twenty-four hours before infection, cells were seeded in sterile 24-well culture plates in Keratinocyte-serum free medium supplemented with 25 µg/mL of bovine pituitary extract and 0.25 ng/mL of epidermal growth factor for keratinocytes, or in Dulbecco's modified eagle medium (DMEM) supplemented with 10%

of fetal bovine serum (FBS) for fibroblasts. Cells were then infected for 1 hour at a MOI of 1 at 37°C in 5% CO_2 in non-supplemented medium. After which, the supernatant was removed, and the cell monolayer was washed with phosphate-buffered saline (PBS) before adding 1 mL of medium followed by an incubation period of 24 or 48 hours. At each time point, supernatants were harvested, and cells were lysed in RA1 lysis buffer from the NucleoSpin RNA extraction kit (Macherey-Nagel).

Ex vivo skin explant infection

After the removal of underlying adipose tissue, small square pieces of skin of 2.25 cm^2 were cut and washed in PBS. Twenty-five microliters of USUV EU2 strain suspension (corresponding to $10^{5,75}$ $TCID_{50}$) was intradermally injected in the center of the skin explant with a 30G insulin syringe. Tissue was placed dermis-side down on 500 µm nylon mesh filtering in 6-well culture plates at the liquid-air interface in 2 mL of DMEM containing 10% FBS and 1% penicillin-streptomycin and incubated at 33°C in 5% CO_2 atmosphere. Cell culture supernatants were collected 24 and 48 hpi to quantify viral replication and production. The central region of explants, corresponding to the inoculation site, was biopsied and lysed in 1 mL of RA1 lysis buffer containing 500 mg of glass beads of diameter ≤ 106 µm followed by four cycles of 20 s at 8,800 rpm using Cryolys tissue homogenizer (Bertin Technologies) or conserved in M-1 Embedding Matrix (Epredia) to perform immunostaining.

Mouse experiments

Six-day-old neonatal Swiss mice (Janvier Laboratories) were inoculated subcutaneously with 10^3 PFU/mice of USUV EU2 or WNV L2 strains (n = 9–13 mice per group). Mouse cutaneous tissues (back, ears, front and back paws, and tail) and spleen were lysed following the protocol used for human skin explants. Mice were bred and maintained according to European institutional (Appendix A STE no. 123) and the French Ministry of Agriculture guidelines.

RNA extraction, reverse transcription and real-time PCR analysis

Total RNA from cell monolayers, skin explant, and murine tissue was isolated using the NucleoSpin RNA Extraction Kit. For viral RNA quantification in cell culture supernatant, 150 µL was extracted using the NucleoSpin RNA Virus Kit (Macherey-Nagel). RNA was quantified using the Nanodrop 2000 spectrophotometer (Thermo Scientific). Total RNA was reverse transcribed using the SuperScript II Reverse Transcriptase Kit (Invitrogen) according to the manufacturer's instructions. To quantify mRNA levels, gene-specific qPCR was carried out using AceQqPCR SYBR Green Master Mix on LightCycler 480 system (Tables S3–S6). Relative mRNA expressions were normalized with two independent housekeeping genes and reported according to the ΔΔCT method as RNA fold increase: $2^{\Delta\Delta CT} = 2^{\Delta CT\ sample\ \Delta CT\ control}$. The calibration ranges for viral quantifications (from 10^4 to 10^{10} cDNA copies/2 µL) were determined using a plasmid containing the 3′UTR of USUV provided by Dr. S. Nisole (IRIM, Montpellier, France) or WNV genome deleted from genes coding structural proteins provided by Dr P. W. Mason (Texas University, Galveston, USA).

Viral titration by endpoint dilution limit method

Vero cells (ATCC CCL-81) were seeded at a density of 2.5×10^3 cells/well in 96-well plates the day before titration, in DMEM supplemented with 2% FBS. One hundred microliters of cell culture supernatants of infected samples was successively diluted from 10^1 to 10^9 in 900 µL of DMEM supplemented with 2% FBS before being deposited in rows of six wells. One hundred microliters of DMEM supplemented with 2% FBS was deposited in a row as a control. A double-blind reading was carried out after 96 hours of incubation at 37°C in an atmosphere containing 5% of CO_2. For each dilution, the wells in which the cells had a cytopathic effect were considered positive for viral infection. The titer of the

viral suspension was then determined using the Spearman-Kärber method for assessing the TCID50/mL.

Quantification of secreted interferons

Levels of biologically active type I IFNs secreted by keratinocytes and fibroblasts were titrated on STING-37 reporter cells as previously described (6). Luciferase induction in STING-37 cells was determined using the Bright-Glo reagent (Promega), according to the manufacturer's instructions, and the luminescence signal was acquired on Infinite 200 pro (Tecan).

Immunofluorescence labeling

Tissues and cells were fixed with 4% paraformaldehyde (PFA), permeabilized for 10 min with 0.3% Triton X-100, and blocked for 30 min with 5% of goat serum. Samples were incubated with primary rabbit anti-dsRNA, mouse anti-pan-*Flavivirus*, or mouse anti-CK10 antibodies and then with secondary goat anti-rabbit or goat anti-mouse antibodies (Table S7). Finally, samples were labeled with DAPI and mounted in DPX Mountant. Images were acquired on an FV3000 confocal microscope (Olympus).

Immunohistochemistry staining

Mouse tissues were fixed in 4% PFA and then embedded in paraffin. Tissues were cut into 3-µm-thick sections, mounted on slides, and then dried at 48°C for at least 30 min. Following deparaffination, the slides were heated for 1 hour at 60°C and subjected to heat-induced antigen retrieval by immersing the slides in 10 mM sodium citrate buffer (pH 6.0) for 30 min at 95°C. After endogenous peroxidase blocking, the slides were incubated with a rabbit anti-dsRNA antibody and then with goat anti-rabbit horse radish peroxidase antibody (Table S7). Visualization of the reaction was achieved using the ImmPACT DAB Substrate Kit (Vector Laboratories). The slides were then counterstained with Harris hematoxylin and dehydrated before coverslips were mounted. A scanner (Aperio GT 450 DX, Leica Biosystems) was used to digitize the slides.

Statistical analyses

The results were analyzed using GraphPad Prism version 5 Software. The statistical significance of the difference between the two groups was evaluated by the nonparametric Mann–Whitney *t* tests and the one-way nonparametric ANOVA test followed by Dunn's test. Differences were considered to be significant when *p* value was less than 0.05.

ACKNOWLEDGMENTS

We thank Anne Cantereau (ImageUp platform of the University of Poitiers) and Clément Jousselin for technical support, and Jeffrey Arsham for the English revision of the paper.

AUTHOR AFFILIATIONS

[1]Laboratoire Inflammation Tissus Epithéliaux et Cytokines (LITEC), Université de Poitiers, Poitiers, France
[2]Pathogenesis and Control of Chronic and Emerging Infections (PCCEI), University of Montpellier, INSERM, EFS, Montpellier, France
[3]Service d'Anatomie et Cytologie Pathologiques, CHU de Poitiers, Poitiers, France
[4]Institut de Recherche en Infectiologie de Montpellier (IRIM), Université de Montpellier, CNRS, Montpellier, France
[5]Department of Virology, Istituto Zooprofilattico Sperimentale dell'Abruzzo e del Molise (IZS-Teramo), Teramo, Italy
[6]Laboratoire de Virologie et Mycobactériologie, CHU de Poitiers, Poitiers, France

AUTHOR ORCIDs

Sébastien Nisole http://orcid.org/0000-0001-9793-419X
Yannick Simonin http://orcid.org/0000-0002-3475-1369
Magali Garcia http://orcid.org/0000-0001-6611-8683
Charles Bodet http://orcid.org/0000-0002-8016-0324

ETHICS APPROVAL

The Ethics Committee of the Poitiers Hospital approved the use of human skin samples for research studies (project identification code: DC-2014-2109). All subjects gave written informed consent in accordance with the Declaration of Helsinki. Experiments were approved by the French Ethics Committee (approval No. 6773-201609161356607).

ADDITIONAL FILES

The following material is available online.

Supplemental Material

Supplemental material (JVI01830-23-S0001.docx). Tables S1 to S7 and Fig. S1.

REFERENCES

1. Pierson TC, Diamond MS. 2020. The continued threat of emerging flaviviruses. Nat Microbiol 5:796–812. https://doi.org/10.1038/s41564-020-0714-0
2. Poidinger M, Hall RA, Mackenzie JS. 1996. Molecular characterization of the Japanese encephalitis serocomplex of the flavivirus genus. Virology 218:417–421. https://doi.org/10.1006/viro.1996.0213
3. Cadar D, Simonin Y. 2022. Human Usutu virus infections in Europe: a new risk on horizon? Viruses 15:77. https://doi.org/10.3390/v15010077
4. Muzumdar S, Rothe MJ, Grant-Kels JM. 2019. The rash with maculopapules and fever in children. Clin Dermatol 37:119–128. https://doi.org/10.1016/j.clindermatol.2018.12.005
5. Garcia M, Wehbe M, Lévêque N, Bodet C. 2017. Skin innate immune response to flaviviral infection. Eur Cytokine Netw 28:41–51. https://doi.org/10.1684/ecn.2017.0394
6. Martin M-F, Maarifi G, Abiven H, Seffals M, Mouchet N, Beck C, Bodet C, Lévèque N, Arhel NJ, Blanchet FP, Simonin Y, Nisole S. 2022. Usutu virus escapes langerin-induced restriction to productively infect human langerhans cells, unlike West Nile virus. Emerg Microbes Infect 11:761–774. https://doi.org/10.1080/22221751.2022.2045875
7. Martin M-F, Nisole S. 2020. West Nile virus restriction in mosquito and human cells: a virus under confinement. Vaccines (Basel) 8:256. https://doi.org/10.3390/vaccines8020256
8. Chessa C, Bodet C, Jousselin C, Wehbe M, Lévêque N, Garcia M. 2020. Antiviral and immunomodulatory properties of antimicrobial peptides produced by human keratinocytes. Front Microbiol 11:1155. https://doi.org/10.3389/fmicb.2020.01155
9. Blázquez A-B, Escribano-Romero E, Martín-Acebes MA, Petrovic T, Saiz J-C. 2015. Limited susceptibility of mice to Usutu virus (USUV) infection and induction of flavivirus cross-protective immunity. Virology 482:67–71. https://doi.org/10.1016/j.virol.2015.03.020
10. Clé M, Barthelemy J, Desmetz C, Foulongne V, Lapeyre L, Bolloré K, Tuaillon E, Erkilic N, Kalatzis V, Lecollinet S, Beck C, Pirot N, Glasson Y, Gosselet F, Alvarez Martinez MT, Van de Perre P, Salinas S, Simonin Y. 2020. Study of Usutu virus neuropathogenicity in mice and human cellular models. PLoS Negl Trop Dis 14:e0008223. https://doi.org/10.1371/journal.pntd.0008223
11. Garcia M, Alout H, Diop F, Damour A, Bengue M, Weill M, Missé D, Lévêque N, Bodet C. 2018. Innate immune response of primary human Keratinocytes to West Nile virus infection and its modulation by mosquito saliva. Front Cell Infect Microbiol 8:387. https://doi.org/10.3389/fcimb.2018.00387
12. Lim P-Y, Behr MJ, Chadwick CM, Shi P-Y, Bernard KA. 2011. Keratinocytes are cell targets of West Nile virus *in vivo*. J Virol 85:5197–5201. https://doi.org/10.1128/JVI.02692-10
13. Surasombatpattana P, Hamel R, Patramool S, Luplertlop N, Thomas F, Desprès P, Briant L, Yssel H, Missé D. 2011. Dengue virus replication in infected human keratinocytes leads to activation of antiviral innate immune responses. Infect Genet Evol 11:1664–1673. https://doi.org/10.1016/j.meegid.2011.06.009
14. Duangkhae P, Erdos G, Ryman KD, Watkins SC, Falo LD, Marques ETA, Barratt-Boyes SM. 2018. Interplay between keratinocytes and myeloid cells drives dengue virus spread in human skin. J Invest Dermatol 138:618–626. https://doi.org/10.1016/j.jid.2017.10.018
15. Hamel R, Dejarnac O, Wichit S, Ekchariyawat P, Neyret A, Luplertlop N, Perera-Lecoin M, Surasombatpattana P, Talignani L, Thomas F, Cao-Lormeau V-M, Choumet V, Briant L, Desprès P, Amara A, Yssel H, Missé D. 2015. Biology of Zika virus infection in human skin cells. J Virol 89:8880–8896. https://doi.org/10.1128/JVI.00354-15
16. Esterly AT, Lloyd MG, Upadhyaya P, Moffat JF, Thangamani S. 2022. A human skin model for assessing arboviral infections. JID Innov 2:100128. https://doi.org/10.1016/j.xjidi.2022.100128
17. Clé M, Constant O, Barthelemy J, Desmetz C, Martin MF, Lapeyre L, Cadar D, Savini G, Teodori L, Monaco F, Schmidt-Chanasit J, Saiz J-C, Gonzales G, Lecollinet S, Beck C, Gosselet F, Van de Perre P, Foulongne V, Salinas S, Simonin Y. 2021. Differential neurovirulence of Usutu viruslineages in mice and neuronal cells. J Neuroinflammation 18:59. https://doi.org/10.1186/s12974-021-02109-y
18. Gaibani P, Cavrini F, Gould EA, Rossini G, Pierro A, Landini MP, Sambri V. 2013. Comparative genomic and phylogenetic analysis of the first Usutu virus isolate from a human patient presenting with neurological symptoms. PLoS One 8:e64761. https://doi.org/10.1371/journal.pone.0064761
19. Cacciotti G, Caputo B, Selvaggi C, la Sala A, Vitiello L, Diallo D, Ceianu C, Antonelli G, Nowotny N, Scagnolari C. 2015. Variation in interferon sensitivity and induction between Usutu and West Nile (lineages 1 and 2) viruses. Virology 485:189–198. https://doi.org/10.1016/j.virol.2015.07.015
20. Fredericksen BL, Keller BC, Fornek J, Katze MG, Gale M. 2008. Establishment and maintenance of the innate antiviral response to West Nile virus involves both RIG-I and MDA5 signaling through IPS-1. J Virol 82:609–616. https://doi.org/10.1128/JVI.01305-07
21. Osterlund PI, Pietilä TE, Veckman V, Kotenko SV, Julkunen I. 2007. IFN regulatory factor family members differentially regulate the expression

of type III IFN (IFN-lambda) genes. J Immunol 179:3434–3442. https://doi.org/10.4049/jimmunol.179.6.3434
22. Rivera-Serrano EE, Gizzi AS, Arnold JJ, Grove TL, Almo SC, Cameron CE. 2020. Viperin reveals its true function. Annu Rev Virol 7:421–446. https://doi.org/10.1146/annurev-virology-011720-095930
23. Lim JK, Lisco A, McDermott DH, Huynh L, Ward JM, Johnson B, Johnson H, Pape J, Foster GA, Krysztof D, Follmann D, Stramer SL, Margolis LB, Murphy PM, Rice CM. 2009. Genetic variation in OAS1 is a risk factor for initial infection with West Nile virus in man. PLoS Pathog 5:e1000321. https://doi.org/10.1371/journal.ppat.1000321
24. Benzarti E, Murray KO, Ronca SE. 2023. Interleukins, chemokines, and tumor necrosis factor superfamily ligands in the pathogenesis of West Nile virus infection. Viruses 15:806. https://doi.org/10.3390/v15030806
25. Schmid MA, Glasner DR, Shah S, Michlmayr D, Kramer LD, Harris E. 2016. Immune cell migration, and dengue pathogenesis during antibody-dependent enhancement. PLoS Pathog 12:e1005676.
26. Turell MJ, Tammariello RF, Spielman A. 1995. Nonvascular delivery of St. Louis encephalitis and venezuelan equine encephalitis viruses by infected mosquitoes (diptera: culicidae) feeding on a vertebrate host. J Med Entomol 32:563–568. https://doi.org/10.1093/jmedent/32.4.563
27. Nemeth N, Young G, Ndaluka C, Bielefeldt-Ohmann H, Komar N, Bowen R. 2009. Persistent West Nile virus infection in the house sparrow (passer domesticus). Arch Virol 154:783–789. https://doi.org/10.1007/s00705-009-0369-x
28. Appler KK, Brown AN, Stewart BS, Behr MJ, Demarest VL, Wong SJ, Bernard KA. 2010. Persistence of West Nile virus in the central nervous system and periphery of mice. PLoS One 5:e10649. https://doi.org/10.1371/journal.pone.0010649
29. Chessa C, Bodet C, Jousselin C, Larivière A, Damour A, Garnier J, Lévêque N, Garcia M. 2022. Antiviral effect of hBD-3 and LL-37 during human primary keratinocyte infection with West Nile virus. Viruses 14:1552. https://doi.org/10.3390/v14071552
30. Huguier V, Giot J-P, Simonneau M, Levillain P, Charreau S, Garcia M, Jégou J-F, Bodet C, Morel F, Lecron J-C, Favot L. 2019. Oncostatin M exerts a protective effect against excessive scarring by counteracting the inductive effect of TGFβ1 on fibrosis markers. Sci Rep 9:2113. https://doi.org/10.1038/s41598-019-38572-0